22PFL-0052

Frequency Coupling Analysis in Spark Ignition Engine Using Bispectral Method and Ensemble Empirical Mode Decomposition

Authors: Ismail El Yacoubi, Stephen Samuel

Abstract

Internal combustion (IC) engines are the current dominant power source used in the automotive industry for hybrid vehicles. The combustion process of IC engines involves various parameters, which are linked to the overall performance of the driveline. Therefore, finding the frequency coupling between the manifold pressure, in-cylinder pressure and output crankshaft speed will provide an insight into the reasons for torque fluctuations and its effect on driveline performance. The present work introduces a methodology to analyze cylinder pressure, manifold pressure and instantaneous crank speed signals measured from a 4 cylinder, 1.6 Litre, Gasoline Direct Injection Engine at different speed conditions to identify the frequency coupling between these signals. This work uses Ensemble Empirical Mode Decomposition (EEMD) as a de-noising method and Bispectral analysis for examining the presence of a frequency coupling from the signals. This paper will demonstrate a systematic approach followed for employing EEMD and Bispectral analysis in a GDI engine for deriving frequency coupling details and its significance.

Introduction

Cylinder pressure is commonly used for deriving the rate of heat release and other combustion related parameters for a given operating conditions in internal combustion (IC) engines [1,2]. Monitoring the characteristics of pressure induced during combustion is a key factor to achieve optimum engine performance. This is given that the pressure from the combustion process of the air-fuel mixture is directly related to output power and torque generated by IC engines [3]. Cylinder pressure signal contains information that can be used in controlling air to fuel ratio balance, fuel Consumption and spark ignition timing [2]. For example, spark ignition timing can significantly affect the torque generated by the engine, as maximum output torque is achieved at a specific spark timing, any advanced or retarded spark timing will result in obtaining a lower torque. This is known as Maximum Brake Torque timing [1]. Therefore, cylinder pressure signal can be used to derive spark timing information for a given air-fuel ratio or any other targeted performance parameters and hence improve the overall output torque and power.

Cylinder pressure signal is generally used for estimating indicated mean effective pressure (IMEP), the location of peak pressure in crank angle (CA) with respect to top dead centre (TDC) of the piston, peak cylinder pressure, mass fraction burned, rate of heat release, cyclic variability, wall heat transfer and many other combustion related details from the time domain cylinder pressure trace. Cylinder pressure information have also been applied to develop closed-loop combustion control algorithms used to optimize fuel injection characteristics [4]. Other uses of cylinder pressure data are found in applications tackling misfire and partial burning issues within Spark ignition engines [5]. However, converting the time domain pressure versus crank angle signal to a frequency domain at a given operating condition allows detecting and characterizing abnormal combustion such as knock in gasoline engines. Engine knocking takes place when the air-fuel mixture auto ignites before being ignited by the spark source and also often due to end gas combustion process which produce a shock wave that results in high frequency and high amplitude pressure oscillations. Its frequency interval is generally between 5 and 7 KHz [6]. A repeated occurrence of heavy knocks can lead to damaging the internal components of an engine such as the exhaust valve, piston and rings. Moreover, noise from constant engine knocking can be unsatisfactory for the vehicle user [6]. Another important signal used in the present work is crankshaft instantaneous speed. This parameter allows a representation of output power feedback and can be used to obtain information on combustion process output. The relationship between cylinder pressure and the output crankshaft rotational speed [7] is well known. Researchers have used signals obtained from crank speed data to reconstruct cylinder pressure signal as a cost-effective approach to replace expensive direct cylinder pressure measurements [7]. Similarly, methods to predict indicated torque using instantaneous crankshaft speed are also found in the literature [8,9]. Various approaches consisting of modelling the relation between crank speed and cylinder pressure parameters using Multi-Layer Perceptron neural network to obtain a non-intrusive cylinder pressure approximation [7] is also gaining more attention recently.

Traditionally, the amount of air inducted per cycle per cylinder or volumetric efficiency, is estimated using intake manifold pressure. Volumetric efficiency, η_v, determines the amount of air inducted per cylinder per cycle and hence the torque generated per cycle. Manifold

pressure has a direct impact on combustion and emissions control [10] and plays an important role in controlling the air-fuel mixture entering the combustion chamber based on the engine operating conditions. Manifold pressure signal is used in the Engine Control Unit (ECU) for estimating mass flow rate of air entering the cylinder and thus adjusting the fuel mixture to meet the torque demand and desired driving conditions [11, 12]. Researchers has also demonstrated the reliability of using intake manifold pressure signal to develop fault diagnosis methods for internal combustion engines [11].

Overall, it can be concluded that the relationship between manifold pressure which directly influences the volumetric efficiency, cylinder pressure resulting from combustion process and the instantaneous crank speed due to torque generated from combustion process are inter-linked and therefore, the analysis of frequency coupling between these signals will allow an optimization of the overall process. Hence, the scope of the current work. Table 1 shows a list of instruments used for measuring manifold pressure, cylinder pressure and crank speed. Whereas, Figure 1, schematically shows the location of sensors.

Table 1: Table of instruments

Data	Measurement instrument
Cylinder pressure	Kistler Spark plug mounted Type 6118C Piezo-electric pressure transducer with the measuring range up to 200 bar
Manifold pressure	Piezoresistive Absolute Pressure Sensor, measurement range of 5 bar, with Amplifier Type 4618A0
Crank instantaneous speed	Rotary Encoder with 360 pulse per rotation with AVL Indiset© Advanced Data Acquisition system

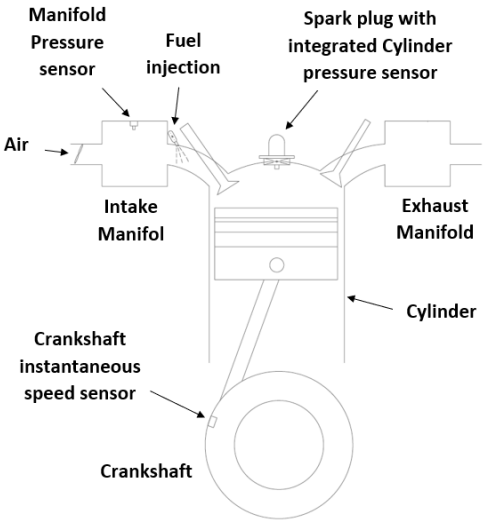

Figure 1: IC engine schematic diagram showing the sensors position to collect cylinder pressure, manifold pressure and instantaneous crank speed datasets.

Signal processing methods

The following section gives brief account of three signal processing methods used in the current work. One of the commonly used signal processing methods for analyzing cylinder pressure is Fast Fourier Transform (FFT). FFT has been widely used to identify the knock and classify the nature of abnormal combustion in cylinder for a long time [13]. However, the main drawback of FFT for combustion application is that, it can identify the presence of various frequency contents in the cylinder pressure signal, but, loses the time resolution and therefore, the location at which the knock occurs can't be identified once the signal is converted to frequency domain using FFT. The location of knock onset is an essential information for optimizing the spark timing and avoiding knock due to auto-ignition of the fuel-air mixture.

Another signal processing method used to overcome this short coming of FFT is Ensemble Empirical Mode Decomposition (EEMD). This is an adaptive method introduced by Wu and Huang [14] and used in analyzing time and frequency data with its suitability for non-linear and non-stationary signals [15]. The principle of this method is to break down the main signal to a set of time domain signals with instantaneous frequencies named Intrinsic Mode Functions (IMF) and a residual signal. An IMF by definition requires meeting two conditions. The first condition is that the number of zero crossings must be equal to or different by one to the number of extrema present within the entire data. Whereas, the second condition requires the resulting mean value of the local minima envelope and local maxima envelope to be zero at any point [16]. Extracting IMFs using EEMD is a process known as sifting algorithm [15]. The following step were proposed by Gaci [15] for extracting IMFs from the original signal for denoising purposes:

1) Find the local minima and maxima (local extrema) of the original signal $x(t)$.

2) Use cubic spline method to complete an interpolation of the local maxima and minima and find the lower $L(t)$ and upper $U(t)$ envelopes.

3) Find the lower and upper envelopes local mean value using: $mean(t) = \frac{U(t)+L(t)}{2}$

4) Subtract $mean(t)$ from the original signal using: $h(t) = x(t) + mean(t)$

5) Use $h(t)$ as a replacement of $x(t)$, then repeat the sifting algorithm steps until finding a signal that meet the two conditions of an IMF defined above.

The number of IMFs obtained from EEMD decomposition is defined after the sifting algorithm ends. The algorithm is stopped once the residual signal ($residual_j(t)$) obtained after the (j-1)th IMF extraction is found to be a monotonic function or if the $residual_j(t)$ is an IMF [16]. In order to re-construct the initial time domain signal, the equation below is used [15]:

$$x(t) = \sum_{j=1}^{j-1} IMF_j(t) + Residual_j(t) \quad (1)$$

EEMD was introduced as an improvement for the original Empirical Mode Decomposition (EMD) approach introduced by Huang et al. [16]. The main advantage of the new EEMD is its ability to overcome the mode mixing issue, which has a common occurrence in EMD. Mode mixing takes place when oscillations of significantly different scales are found in any resulting IMF after decomposition, which can result in the loss or faults in physical meanings associated with IMFs [14]. The way EEMD differs from EMD and solves mode mixing problems is through adding white noise to the original signal. This noise acts as a reference scale distribution resulting in a much simpler EMD process. After the added white noise serves its function in reducing the risk of mode mixing, it is cancelled out in the calculation of the last mean of each IMF [14].

EEMD also proved to be an effective signal de-noising method. The general methodology followed to remove noise from a signal using EEMD is through decomposing the time domain, identifying and eliminating IMFs representing unwanted noise, then re-composing the signal using equation 1. The high frequency noise within the decomposed signal is generally present within lower order IMFs. Whereas, the energy of noise decreases with the increase of the IMFs order number [14]. Hence, the boundary of IMFs representing noise can be found by identifying the IMF containing the lowest high frequency noise proportion. Zhang and Wei [17] introduced a methodology to identify the boundary of IMFs containing noise. This method consists of the following steps:

1) Computing the standard deviation of an IMF by using the following formula:

$$\sigma_i = \sqrt{\frac{1}{N-1}\sum_{j=1}^{N}\left(IMF_i(j) - \overline{IMF_i(j)}\right)^2} \qquad (2)$$

In equation 2, N represents the IMF data length and 'i' corresponds to the IMF order number.

2) Computing the noise standard deviation for the corresponding IMF using the equation below:

$$\hat{\sigma}_i = \frac{median\left(\left|IMF_i(j) - \overline{IMF_i(j)}\right|\right)}{0.6745} \qquad (3)$$

Similar to Equation 2, variable 'i' in equation 3 represents the IMF order number.

3) Evaluate the boundary of IMFs representing noise using:

$$K = \frac{argmax\left(\frac{\sigma_i}{\hat{\sigma}_i}\right) + argmax\left(\sigma_i - \hat{\sigma}_i\right)}{2} \qquad (4)$$

IMFs representing noise are identified as any IMFs with an order number smaller or equal to K.

For example, figure 2 shows a signal y(x) to which noise has been added compared with the de-noising process outcome. By applying EEMD using R© 3.6.3 Rlibeemd package, signal y(x) can be decomposed to the IMFs illustrated in figure 3. IMFs 1 to 3 were identified as unwanted high frequency noise using Zhang and Wei [17] method described above, and hence by summing IMFs 4 to 7 and residual, the noise free y(x) signal is obtained.

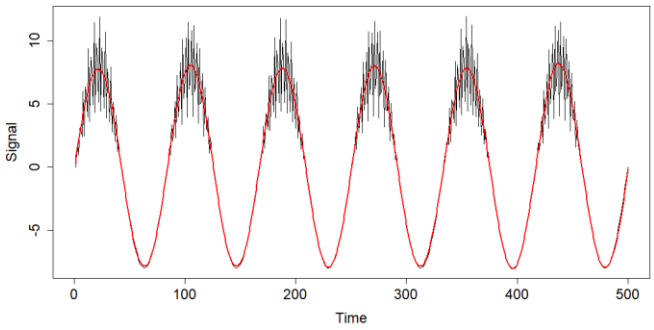

Figure 2: An example of signal y(x) generated with added noise (Black line) compared with the de-noised signal (Red line) after applying EEMD

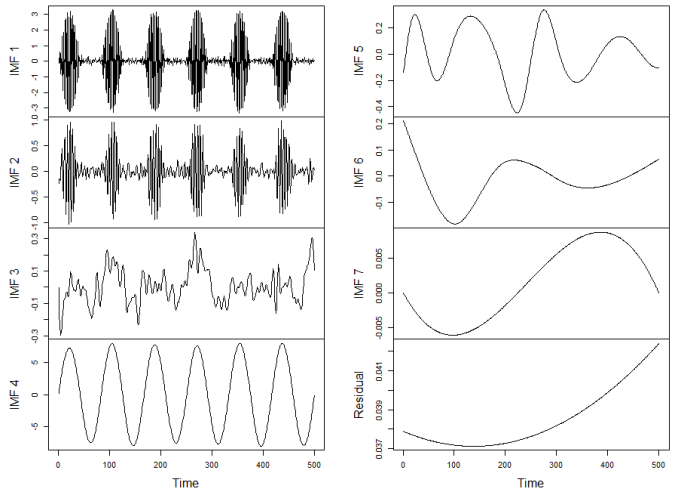

Figure 3: IMFs obtained after EEMD decomposition process of signal y(x)

The third method used is Higher Order Spectral Analysis (HOSA). This is an approach originally used in statistical analysis and can be represented as the $(n-1)$th Fourier Transform of n^{th} order sequences [18]. This method is ideal for non-linear and non-Gaussian signal analysis along with its ability to identify correlation or phase coupling in time series. Whereas, the 2nd order Fourier transformation of a time domain's 3rd order cumulants is identified as bispectrum, which can be found using the following equation [19,20]:

$$B(f_1, f_2) = \frac{1}{T}\sum_{t=0}^{T} X_t(f1)\, X_t(f2) X_t^*\,(f1+f2) \qquad (5)$$

$$B(f_1, f_2) = E[X_t(f1) X_t(f2) X_t^*\,(f1+f2)] \qquad (6)$$

Where X_t is the Fourier transform of the t-th segment of X_t and T is the total number of segments, X_t^* is its complex conjugate and *f1*, *f2 and (f1+f2)* are three individual frequency components while the expectation is represented by E. When these three frequency components are non-linearly coupled to each other, the total phase of these three components will be strongly correlated even though each of the induvial phases are random.

An illustration for bispectrum borrowed from [21] is shown in Figure 4. When two independent frequencies derived from the decomposed signals are plotted as x and y axis, the third component due to interaction between these two frequencies which represent the bispectral quantity can be located.

Bispectral analysis has found its application in various fields such as speech analysis [21], fault diagnostics of vibration data [20], wave analysis [22], underwater acoustics [18], sonar data [23], detecting forgery [24], musical [25], medical application [19] and many more. This signal processing method will be employed in the present work.

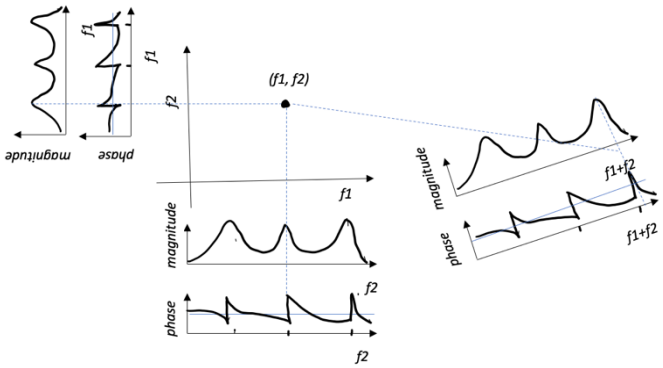

Figure 4: An example re-drawn from [21] illustrating the principle of Bispectrum method in measuring the frequencies and interactions between multiple signals

Scheme of work

Experimental process

The specifications of the engine used for measuring manifold pressure, cylinder pressure and instantaneous crank speed are shown Table 2.

Table 2: Specifications of Experimental engine

Parameter	**Value**
Bore diameter	77 mm
Stroke length	85.8 mm
Connecting rod length	138.4 mm
Number of cylinders	4
Compression ratio	10.5
Fuel injection type	Gasoline Direct injection
Induction type	Turbocharged and intercooled

In order to collect the required data, two piezoelectric transducers were used to measure cylinder pressure and manifold pressure of the engine. Crank angle encoder connected to the crankshaft at the pulley end was used to measure the instantaneous crank speed. AVL Indiset© advanced data logging system was used for collecting and analyzing these data.

Signal post processing methodology

Once the time domains data are obtained, signal post processing methods can be used to analyze these three datasets, manifold pressure, cylinder pressure and instantaneous crank speed measured as function of crank angle with one degree crank angle interval. FFT was first used as a method to convert the time domains to frequency domains using MATLAB programming software for the purpose of extracting the main dominant frequencies. Once this is completed, EEMD is applied for de-noising the time domains along with decomposing the original signals to multiple IMFs using R© 3.6.3 Rlibeemd package. The de-noising process applies the following equation:

$$Y(t) = \sum_{j=n+1}^{j-1} IMF_j(t) - \sum_{j=1}^{n} IMF_j(\mathrm{t}) + Residual_j(\mathrm{t}) \qquad (7)$$

The concept of equation 7 is to eliminate n number of *IMFs* which represent unwanted noise then recomposing the signal by adding the rest of the IMFs and residual.

Once EEMD analysis outcome is obtained, Bispectral analysis is used to study the frequency coupling between cylinder pressure, manifold pressure and crank instantaneous speed. HOSA outcome is represented as Bispectrum and Bicoherence graphs in order to identify the frequency coupling between manifold pressure, cylinder pressure and instantaneous crank speed signals.

Results and discussion

Figures 5(a) illustrates the cylinder pressure signal at firing condition obtained at 1600 rev/min and 40 Nm. The spark timing and IMEP of the pressure data presented in figure 5(a) are 36º before TDC and 3.6 bar, respectively. The noise present within the compression and expansion stroke of cylinder pressure data is due to the opening and closing of inlet and exhaust valves events, spark ignition noise and fuel injection noise. Whereas, figures 5(b) and 5(c) illustrate the signals obtained for manifold pressure and crank instantaneous speed at 1600 rev/min and 40 Nm. The experimental data used for this work are based on the average of 13 engine cycles. It can be observed that these signals contain multiple frequencies. Hence, the time domains are converted to frequency domains via FFT method in order to find the dominant frequencies. The resulting FFT plots are demonstrated in figures 6(a), 6(b) and 6(c).

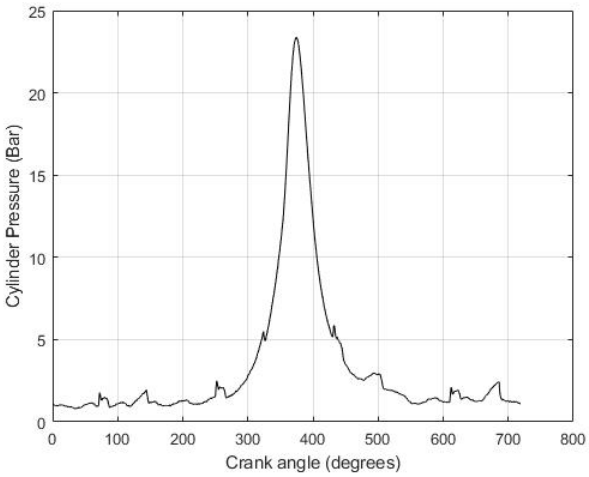

Figure 5(a): Cylinder pressure data of one cylinder at engine speed of 1600 rpm, load 40 N.m

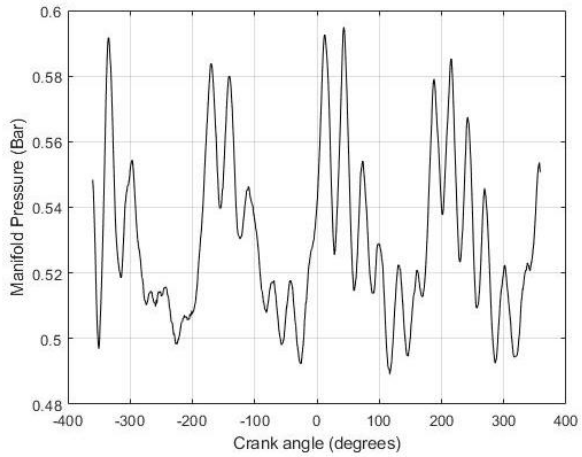

Figure 5(b): Manifold pressure obtained signal at engine speed of 1600 rpm and load 40 N.m

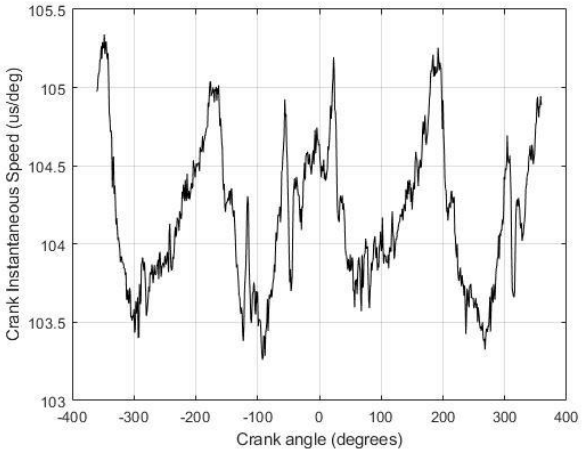

Figure 5(c): Crank instantaneous speed obtained signal at engine speed of 1600 rpm and load 40 N.m

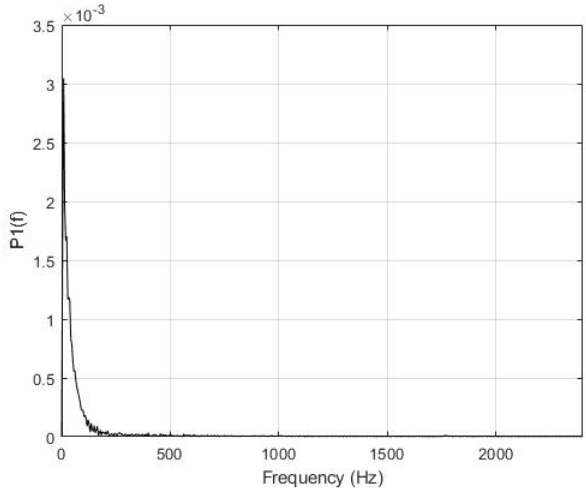

Figure 6(a): FFT of cylinder pressure at engine speed of 1600 rpm and load 40 N.m

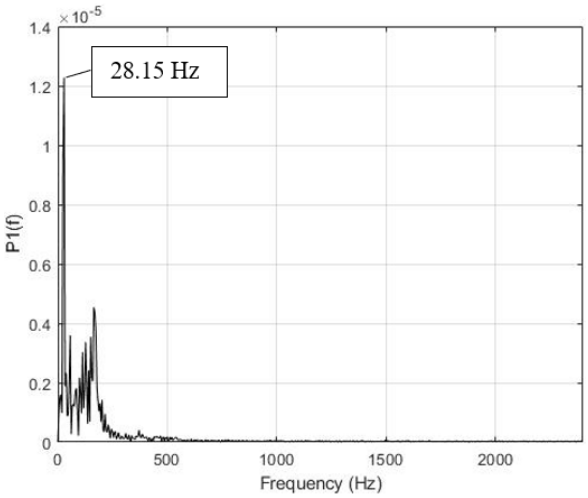

Figure 6(b): FFT of manifold pressure at engine speed of 1600 rpm and load 40 N.m

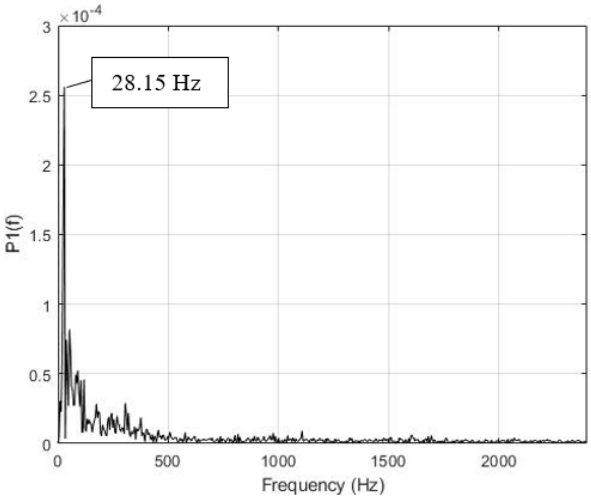

Figure 6(c): FFT of crank instantaneous speed signals at engine speed of 1600 rpm and load 40 N.m

It is seen from FFT results that the dominant frequencies are mainly in the first region between 0 and 500 Hz. In order to get more information from the plots shown in figures 6(a), 6(b) and 6(c), the main peaks found in FFT graphs are extracted to be compared in figure 7. It can be seen that some similar frequency values are present within the signals obtained. For example, the frequency 28.15 Hz is present in both manifold pressure and crank instantaneous speed FFT plots. This frequency also has the highest energy based on the results in figures 6(b) and 6(c), 28.15 Hz represents the main crankshaft speed and is also found in the manifold pressure signal.

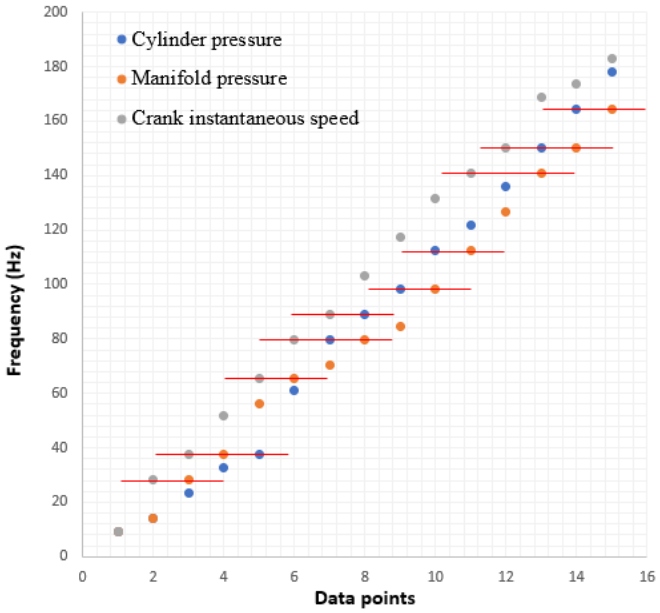

Figure 7: A comparison between the main frequencies extracted from FFT results at engine speed of 1600 rpm and load 40 Nm showing some matching frequency values within the signals measured

Ensemble Empirical Mode Decomposition

By applying EEMD to cylinder pressure data, the resulting IMFs after the decomposition process are illustrated in figure 8.

IMFs 1 to 3 are found to represent noise within in the original signal. Hence, the first three IMFs are not considered and eliminated to remove noise from cylinder pressure recorded data. Hence, by summing the rest of the IMFs and residual. The de-noised cylinder pressure signal is obtained and demonstrated in figure 9.

In order to analyze the frequencies within the measured data, the firing frequency of the experimental engine used in this work is considered. The overall firing frequency for IC engines is dependent on the speed at which the engine is running and the number of cylinders. The combustion process within each cylinder results in a power delivery pulse corresponding to a certain frequency. The overall engine firing frequency can then be obtained as the frequency value of the power pulse produced by each cylinder multiplied by the total number of cylinders. Hence, the engine firing frequency (f_c) can be expressed as [27]:

$$f_c = \frac{N \times n}{60 \times k} \quad (8)$$

The parameters N, n and k represent the engine speed in rpm, number of engine cylinders and the number of revolutions per cycle, respectively. In this case, the number of cylinders is four and the crankshaft completes two revolutions per cycle for the four-stroke experimental engine used in this project, i.e. $n = 4$ and $k = 2$. Hence, the engine firing frequency value obtained using equation 8 considering one cylinder only at 1600 rpm is 13.34 Hz. Whereas, the firing frequency considering all 4 cylinders is found to be 53.34 Hz.

In order to extract present features of the signals within its IMFs, FFT is used to obtain the frequency domain of these IMFs. Similar approach has been used in other applications found in the literature [26]. This was achieved through decomposing raw signals to IMFs using EEMD and then producing the power spectrum of these IMFs using FFT to extract features or events representing system dynamics found in raw signals. This method has direct applications in the present work and can be applied for the IMFs obtained from the decomposition process of cylinder pressure, manifold pressure and crank instantaneous speed.

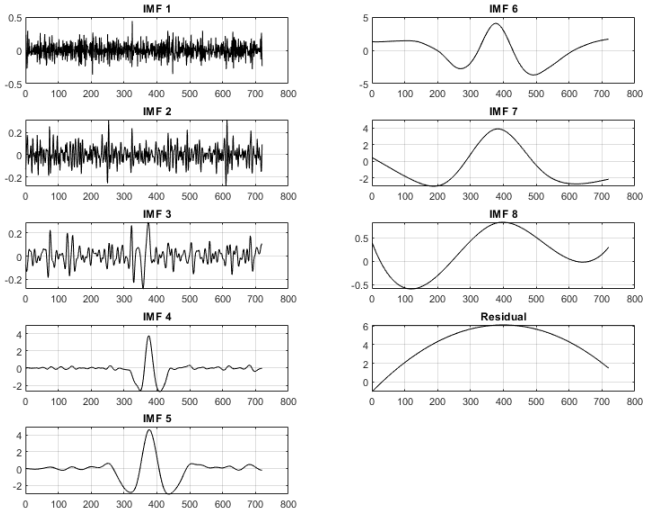

Figure 8: IMFs of Cylinder pressure signal at engine speed of 1600 rpm and load 40 N.m

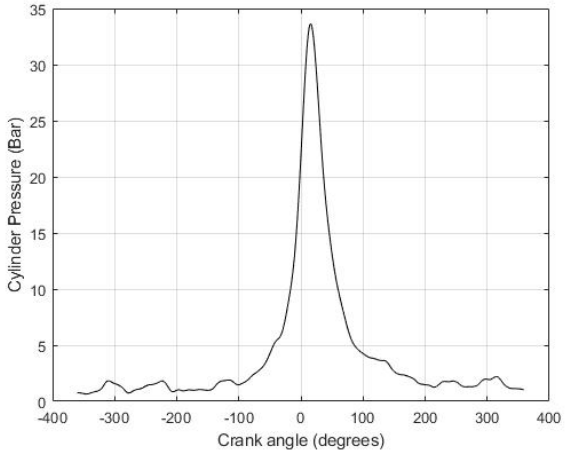

Figure 9: De-noised cylinder pressure signal

Figure 10 shows the FFT results of cylinder pressure signal IMFs. From the FFT plot of IMF 6, it is noticed that EEMD detected a critical combustion event present in IMF 6 corresponding to a peak frequency value of 14.08 Hz. This frequency value is very close to the theoretical engine firing frequency value of 13.34 Hz considering one cylinder at an engine speed of 1600 rpm. FFT was also applied to cylinder pressure data IMFs at 2000 rpm, the FFT of IMF 6 of this speed condition is illustrated in figure 11. The results in figure 11 show a peak at 18.77 Hz which is close to the engine firing frequency at 2000 rpm. The theoretical firing frequency in this case considering one cylinder is 16.67 Hz. Therefore, it can be concluded that cylinder pressure IMF 6 represent the engine firing event during combustion.

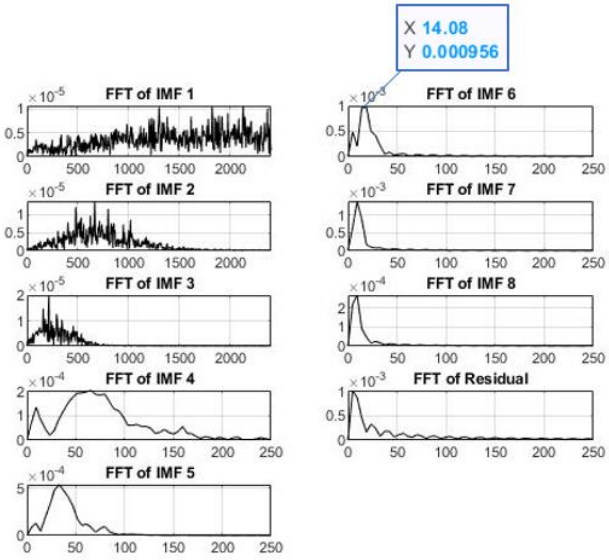

Figure 10: FFT of cylinder pressure IMFs at engine speed of 1600 rpm and load 40 Nm

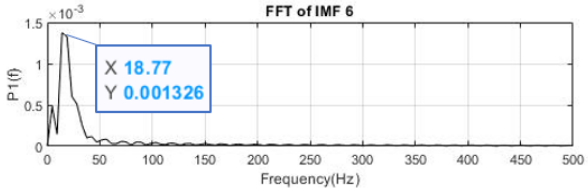

Figure 11: FFT of IMF 6 obtained from EEMD decomposition of cylinder pressure data at engine speed of 2000 rpm and load 40 Nm

EEMD process was applied to manifold pressure, and the resulting denoised time domain is illustrated in figure 12. It can be noticed that changes to the manifold pressure signal due to the denoising process are very minimal, which shows that the noise energy detected in the original data is very low. The same method is applied to crank instantaneous speed signal as shown in figure 13 where the resulting time domain after EEMD is compared to the original recorded signal.

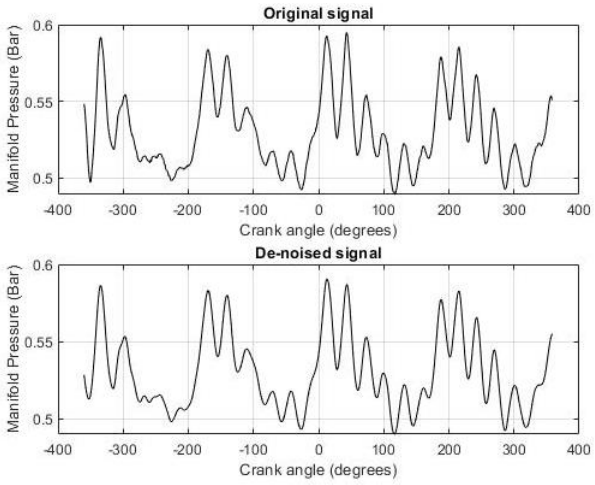

Figure 12: A comparison between the original and de-noised manifold pressure signal

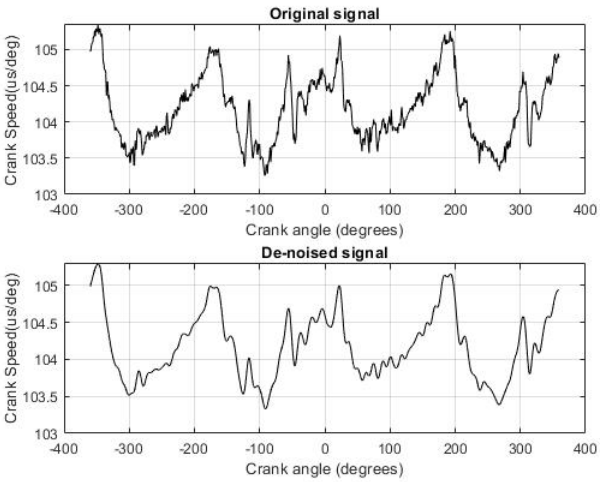

Figure 13: A comparison between the original and de-noised crank instantaneous speed signal

However, EEMD is limited when it comes frequency coupling and is unable to detect the presence of a coupling or correlation between multiple signals. This objective is completed using Bispectral analysis, as this method is capable of extracting the coupling between these frequencies.

Higher Order Spectral Analysis

Higher order spectral analysis is based on various analytical strategies such as cross-bispectrum, which by considering three time domain signals can be expressed by the following triple product [28]:

$$B_{123}(z_1, z_2) = X_1(z_1) \times X_2(z_2) \times X_3(z_1^{-1} \times z_2^{-1}) \qquad (9)$$

$X_n(z)$ represents signal $x_n(a)$ transform with n being 1,2 or 3.

Bispectrum analysis of a particular time domain signals is estimated following two methods. The main one is the use of direct FFT process for the estimation. This process is based on the principle of equation 9, with an option for smoothing the frequency domain via Roa-Gabr window [29]. The second method is estimating bispectrum

via the indirect method, which consists of dividing the signal to segments with possible overlapping events. For each of these events, a computation of unbiased sample estimates of their 3rd order cumulants is executed. The next stage is to average these sample estimates across events [18]. In the present work, MATLAB functions bispecdx and bispeci from HOSA package are used to obtain the combustion signals cross-bispectrum via direct FFT and indirect method, respectively. Cross-bispectrum plots are originally 3D graphs. However, they are represented in 2D with the colors of the contours signifying the z-axis level of the plots. The yellow contours represent the highest level of coupling while purple is the lowest level. Figures 14 and 15 show bispectrum results for engine speed of 1600 rpm and 40 Nm load. It can be seen that the resulting contours are different from zero, which signifies the presence of a coupling between cylinder pressure, manifold pressure and crank instantaneous speed. It is also noticed that the cross-bispectrum estimation has a peak corresponding to an $f1$ value of around 0.005568 and an $f2$ value of around 0.002966. These two frequencies are linked together by a third frequency $f3$ with the relation expressed as:

$$f_3 = f_1 + f_2 \tag{10}$$

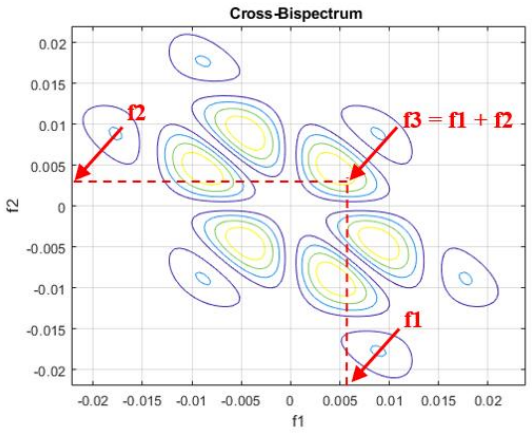

Figure 14: Cross-Bispectrum plot via direct method of cylinder pressure, manifold pressure and crank instantaneous speed at engine speed of 1600 rpm and load 40 Nm showing the locations of f1, f2 and f3

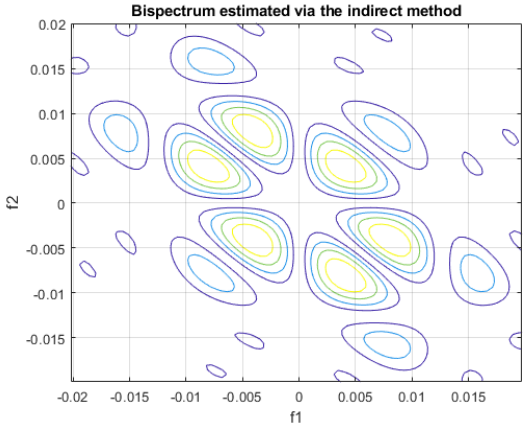

Figure 15: Cross-Bispectrum plot via indirect method of cylinder pressure, manifold pressure and crank instantaneous speed at engine speed of 1600 rpm and load 40 N.m

Whereas, the physical explanation of equation 10 concept is that f_1 is a frequency corresponding to an event in cylinder pressure signal, f_2 to a manifold pressure event, while f_3 is corresponding an event in crank speed signal. The negative frequencies shown in the bispectrum plots are the complex conjugate of their reflections [18,30].

The resulting frequencies from bispectrum plots are given as normalized frequencies. Therefore, equation 11 below is used to obtain the frequency values in Hz:

$$f_{Hz} = f_n \times f_s \tag{11}$$

f_n and f_s represent the normalised frequency and sampling frequency, respectively.

Hence, the cross bispectrum peak corresponding to 0.005568 + 0.002966 = 0.008478 can be expressed as 53.45 Hz + 28.48 Hz = 81.93 Hz. It is noticed that the frequency f_1 of 53.45 Hz has a close value to the engine firing frequency, which has a theoretical value of 53.33 Hz. It is also seen that the frequency value of $f_2 = 28.48\ Hz$ is close to 28.15 Hz which is a frequency with the highest energy in crank instantaneous speed and manifold pressure signal based on the results in figure 6(b) and 6(c) obtained from FFT analysis. Whereas, $f_3 = 81.93\ Hz$ is close to one of the main frequency peaks with a value of 79.77 Hz extracted from crank instantaneous speed FFT plot as shown in figure 7.

Figures 16 and 17 show the bispectrum results obtained at engine speed of 2000 rpm and 40 Nm load. It can be seen that these contour plots show multiple peaks. This signifies that a frequency coupling is also present at 2000 rpm.

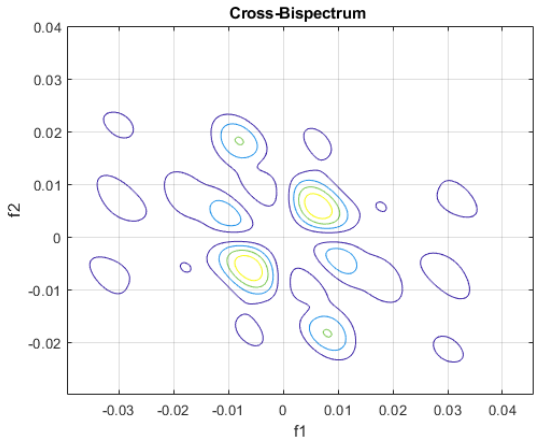

Figure 16: Cross-Bispectrum plot via direct method of cylinder pressure, manifold pressure and crank instantaneous speed at engine speed of 2000 rpm and load 40 Nm

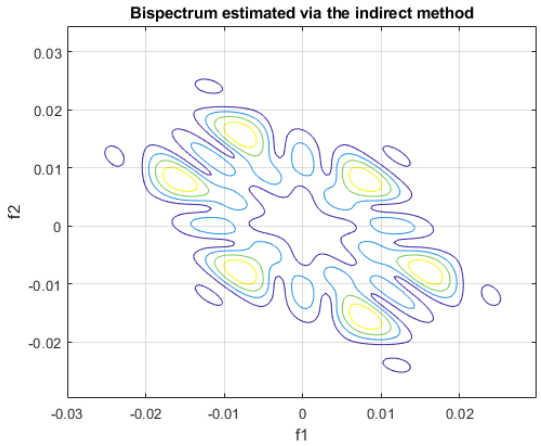

Figure 17: Cross-Bispectrum plot via indirect method of cylinder pressure, manifold pressure and crank instantaneous speed at engine speed of 2000 rpm and load 40 Nm

Bicoherence results

Bicoherence is a very useful process in higher order spectral analysis to examine nonlinearities found in time domain signals [30], which makes this analysis strategy suitable for extracting quadratic phase coupling present within a particular signal. The theoretical expression followed to obtain bicoherence estimation is as shown in the following equation [30]:

$$Bicoherence\ (f_1, f_2) = \frac{|B(f_1, f_2)|^2}{A\{|X(f_1) \times X(f_2)|^2\} \times A\{|X(f_1 + f_2)|^2\}} \quad (12)$$

$B(f1, f2)$ represents the bispectrum calculation using equation 5. While $X(f)$ refers to the Fourier transformation procedure. Parameter 'A' in equation 12 is an averaging operator and can be expressed as:

$$A(F) = \frac{1}{T}\sum_{t=0}^{T} F^{(j)} \quad (13)$$

'F' represents derived quantities such as the Fourier transform of the t-th segment of X_t. Whereas, T is the total number of segments as explained in equation 5.

Bicoherence analysis is used in the present work as an additional HOSA procedure to examine presence of frequency coupling within the combustion signals and compare these results with the outcome obtained from cross-bispectrum analysis. The results of bicoherence analysis are illustrated in figures 18 and 19 below.

The results show that maximum bicoherence values of 0.89 and 0.47 has been obtained for engine speeds of 1600 rpm and 2000 rpm, respectively. These values are different from zero which signifies the presence of a frequency coupling in both speed conditions.

However, certain limitations were found in bispectral analysis during the present work. The main overall drawback of HOSA is the long computation timing required to complete the desired analysis, this can negatively affect the cost of undertaking such heavy computational process for professional and industrial use of this analytical approach. The present work draw only attention to firing frequency in order to demonstrate the application of bispectral analysis for GDI engine, however, further analysis could reveal frequency coupling between other dynamic processes and their physical relevance.

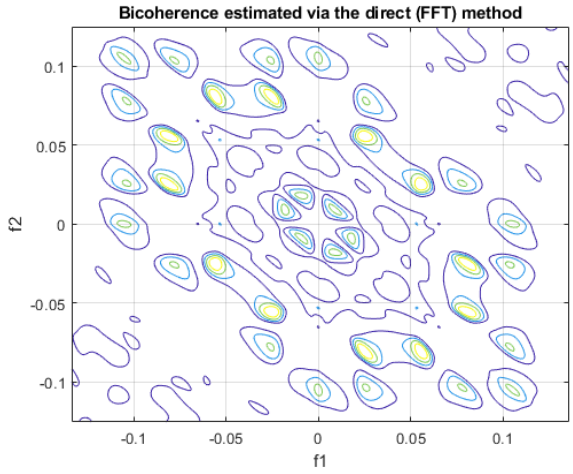

Figure 18: Bicoherence estimation results based on direct FFT method speed at engine speed of 1600 rpm and load 40 Nm

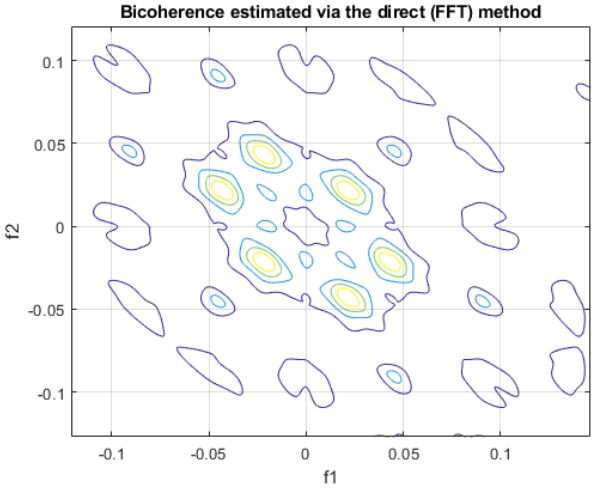

Figure 19: Bicoherence estimation results based on direct FFT method at engine speed of 2000 rpm and load 40 Nm

Conclusions

This paper presents a methodology to analyze critical parameters related to internal combustion engines performance using Bispectral analysis and EEMD. This method proved its suitability to preserve time information and signal features during the analysis, overcome the mode mixing issue associated with the original EMD and to detect frequency coupling features. This method is applied to cylinder pressure, manifold pressure and crank instantaneous speed data measured from a 4 cylinder, 1.6 Litre, Gasoline Direct Injection Engine in order to find the frequency coupling within these signals. The choice of these parameters was based on the direct relation of IC engines performance, output power and volumetric efficiency with

these three signals as demonstrated by background literature. EEMD was used to decompose the signals into a set of IMFs. The results after the decomposition process show that IMF 6 of cylinder pressure data was correlated with the theoretical firing frequency of the cylinder at 1600 rpm and 2000 rpm. Whereas, bispectrum and bicoherence results show the presence of a frequency coupling between cylinder pressure, manifold pressure and crank instantaneous speed at engine speeds of 1600 rpm and 2000 rpm with a load of 40 Nm. At 1600 rpm, the coupled frequencies f1, f2 and f3 were compared to FFT and EEMD outcome and the comparison showed that f1 corresponds to the engine firing frequency, f2 to the engine speed found after the computation of manifold pressure and crankshaft instantaneous speed FFT, while f3 corresponds to a frequency of 81.93 Hz close to a frequency value found in crankshaft instantaneous speed FFT. This method can be used to identify other signal features and frequency couplings present between combustion, crankshaft and other connected driveline components of vehicle systems.

References

1. Heywood, J., *Internal Combustion Engine Fundamentals*, 1st ed. (New York [etc.]: McGraw-Hill, 1988), 1-10, ISBN: 0-07-028637-X.

2. Sellnau, M., Matekunas, F., Battiston, P., Chang, C., et al., "Cylinder-Pressure-Based Engine Control Using Pressure-Ratio-Management and Low-Cost Non-Intrusive Cylinder Pressure Sensors," SAE Technical Paper 2000-01-0932, 2000, doi: 10.4271/ 2000-01-0932.

3. Doggett, W., “Measuring Internal Combustion Engine In-Cylinder Pressure with LabVIEW,” National Instruments 2010, USA, Jun 28, 2010.

4. Jorques Moreno, C., Stenlåås, O., and Tunestål, P., “In-Cycle Closed-Loop Combustion Control with Pilot-Main Injections for Maximum Indicated Efficiency,” *IFAC-PapersOnLine* 51 (31): 92-98, 2018, doi: 10.1016/j.ifacol.2018.10.018.

5. Cesario, N., Tagliatatela, F., and Lavorgna, M., “Methodology for Misfire and Partial Burning Diagnosis in SI Engines,” *IFAC Proc.* 39 (16): 1024-1028, 2006, doi: 10.3182/20060912-3- DE-2911.00176.

6. Horner, T., "Knock Detection Using Spectral Analysis Techniques on a Texas Instruments TMS320 DSP," SAE Technical Paper 960614, 1996, doi: 10.4271/960614.

7. Taglialatela, F., Lavorgna, M., Mancaruso, E., and Vaglieco, B., “Determination of combustion parameters using engine crankshaft speed,” *Mechanical Systems and Signal Processing* 38 no. 2 (2013): 628–633, doi: 10.1016/j.ymssp.2012.12.009.

8. Rizzoni, G., "Diagnosis of individual Cylinder Misfires by Signature Analysis of Crankshaft Speed Fluctuations," SAE Technical Paper 890884, 1989, doi: 10.4271/890884.

9. Citron, S., O'Higgins, J., and Chen, L., "Cylinder by Cylinder Engine Pressure and Pressure Torque Waveform Determination Utilizing Speed Fluctuations," SAE Technical Paper 890486, 1989, doi: 10.4271/890486.

10. Tsironas, S., Stenlaas, O., Apell, M., and Cronhjort, A., “Heavy-Duty Engine Intake Manifold Pressure Virtual Sensor,” SAE Technical Paper 2019-01-1170, 2019, doi: 10.4271/2019-01-1170.

11. Wu, J., Huang, C., Chang, Y., and Shiao, Y., “Fault diagnosis for internal combustion engines using intake manifold pressure and artificial neural network,” *Elsevier* 37 no. 2 (2010): 949-958, doi: 10.1016/j.eswa.2009.05.082.

12. Reß, J., Bohn, C., Märzke, F., Meinecke, R. et al., "Inversion-Based Intake Manifold Pressure Control System for Modern Diesel Engines," SAE Int. J. Engines 7(3):1539-1546, 2014, doi: 10.4271/2014-01-1709.

13. Kirsten, M., Pirker, G., Redtenbacher, C., Wimmer, A. et al., "Advanced Knock Detection for Diesel/Natural Gas Engine Operation," SAE Int. J. Engines 9(3): 1571-1583, 2016, doi: 10.4271/2016-01-0785.

14. Wu, Z., and Huang, N., “Ensemble Empirical Mode Decomposition: A Noise-Assisted Data Analysis Method,” *World Scientific* 1 no. 1 (2009): 1-41, doi: 10.1142/S1793536909000047.

15. Gaci, S., “A New Ensemble Empirical Mode Decomposition (EEMD) Denoising Method for Seismic Signals,” *Energy Procedia* 97 (2016): 85-91, doi: 10.1016/j.egypro.2016.10.026.

16. Huang, N., Shen, Z., Long, S., Wu, M., et al., “The Empirical Mode Decomposition and the Hilbert Spectrum for Nonlinear and Non-Stationary Time Series Analysis”, *the Royal Society Publishing* 454 (1971): 903-995, doi: 10.1098/rspa.1998.0193.

17. Zhang, M., and Wei, G., “An integrated EMD adaptive threshold denoising method for reduction of noise in ECG,” *PLoS ONE* 15 no. 7 (2020), doi: 10.1371/journal. pone.0235330.

18. Morella, G., “A Review of Signal Detection Using the Bispectrum with Applications in Underwater Acoustics,” *The Pennsylvania State University*, January 1994. Available at: https://apps.dtic.mil/dtic/tr/fulltext/u2/a275227.pdf

19. Sharmila, K., Krishna, E., Komalla, N., Reddy, K., “Use of higher order spectral analysis for the identification of sudden cardiac death”, *IEEE* (2012), doi: 10.1109/MeMeA.2012.6226674.

20. Halim, E., Choudhury, M.., Shah, S., and Zuo, M., “Fault detection of Rotating Machinery from Bicoherence Analysis of Vibration data,” *IFAC Proceedings* 39 no. 13 (2006): 1348-1353, doi: 10.3182/20060829-4-CN-2909.00225.

21. Fackrell, J., “Bispectral Analysis of Speech Signal,” Ph.D. thesis, The University of Edinburgh, 1996.

22. Cherneva, Z., Andreeva, N., Petrova, P., “Bi-spectral analysis of wind wave in the Black Sea coastal zone,” Paper presented at 7th International Conference on Marine Sciences and Technologies Black Sea 2004, Varna, Bulgaria, October 7-9, 2004.

23. Persson, L., Lennartsson, R., Robinson, J., and McLaughlin, S., "Quadratic phase coupling analysis of passive sonar data using biphase techniques," OCEANS 2000 MTS/IEEE Conference and Exhibition. Conference Proceedings (Cat. No.00CH37158),

2000, pp. 1053-1057 vol.2, doi: 10.1109/OCEANS.2000.881740.

24. Hany, F.," Detecting Digital Forgeries Using Bispectral Analysis" AIM-1657, 1999, https://dspace.mit.edu/handle/1721.1/6678, [Accessed 21 Dec 21]

25. Dubnov, S., "Polyspectral Analysis of Musical Timbre,", Ph.D. Thesis, Hebrew University, 1996.

26. Tjandrasa, H., Djanali, S., and Arunanto, F., "Feature Extraction Using Combination of Intrinsic Mode Functions and Power Spectrum for EEG Signal Classification", *IEEE* (2016), doi: 10.1109/CISP-BMEI.2016.7852954.

27. Archer, A. and McCarthy Jr, J., "Quantification of Diesel Engine Vibration Using Cylinder Deactivation for Exhaust Temperature Management and Recipe for Implementation in Commercial Vehicles," SAE Technical Paper 2018-01-1284, 2018, doi: 10.4271/2018-01-1284.

28. Brooks, D., and Nikias, C., "The Cross-Bicepstrum: Definition, Properties, and Application for Simultaneous Reconstruction of Three Nonminimum Phase Signals," *IEEE Transactions on Signal Processing* 41 no. 7 (1993): 2389-2404, doi: 10.1109/78.224248.

29. Roa, T., and Gabr, M., *An Introduction to Bispectral Analysis and Bilinear Time Series Models*, 1st ed. (New York, NY: Springer US, 1984), ISBN: 978-1-4684-6318-7.

30. Newman, J., Pidde, A., and Stefanovska, A.," Defining the wavelet bispectrum, Applied and Computational Harmonic Analysis, Volume 51, March 2021, Pages 171-224

31. Poloskei, P., Papp, G., Por, G., Horvath, L., et al., "Bicoherence analysis of nonstationary and nonlinear processes," ArXiv, November 2018. Available at: https://arxiv.org/pdf/1811.02973.pdf

Definitions/Abbreviations

IC – Internal Combustion

IMEP – Indicated Mean Effective Pressure

CA – Crank Angle

TDC – Top Dead Centre

FFT – Fast Fourier Transform

EMD – Empirical Mode Decomposition

EEMD – Ensemble Empirical Mode Decomposition

IMF – Intrinsic Mode Function

HOSA – Higher Order Spectral Analysis